

# Two critical temperatures conundrum in $\text{La}_{1.83}\text{Sr}_{0.17}\text{CuO}_4$

Abhisek Samanta<sup>1</sup>, Itay Mangel<sup>2</sup>, Amit Keren<sup>2</sup>, Daniel P. Arovas<sup>3</sup>, Assa Auerbach<sup>2</sup>

<sup>1</sup> Department of Physics, The Ohio State University, Columbus OH 43210, USA,

<sup>2</sup> Physics Department, Technion, Haifa, Israel

<sup>3</sup> Department of Physics, University of California at San Diego,  
La Jolla, California 92093, USA

\*Corresponding: assa@physics.technion.ac.il

January 30, 2024

## Abstract

The in-plane and out-of-plane superconducting stiffness of  $\text{La}_{1.83}\text{Sr}_{0.17}\text{CuO}_4$  rings appear to vanish at different transition temperatures, which contradicts thermodynamical expectation. In addition, we observe a surprisingly strong dependence of the out-of-plane stiffness transition on sample width. With evidence from Monte Carlo simulations, this effect is explained by very small ratio  $\alpha$  of interplane over intraplane superconducting stiffnesses. For three dimensional rings of millimeter dimensions, a crossover from layered three dimensional to quasi one dimensional behavior occurs at temperatures near the thermodynamic transition temperature  $T_c$ , and the out of-plane stiffness *appears* to vanish below  $T_c$  by a temperature shift of order  $\alpha L_a/\xi^{\parallel}$ , where  $L_a/\xi^{\parallel}$  is the sample's width over coherence length. Including the effects of layer-correlated disorder, the measured temperature shifts can be fit by a value of  $\alpha = 4.1 \times 10^{-5}$ , near  $T_c$ , which is significantly lower than its previously measured value near zero temperature.

## 1 Introduction

A homogeneous three-dimensional superconductor is expected to exhibit a single transition temperature  $T_c$  at which the order parameter,  $\Delta(T)$ , and all the superconducting stiffness components vanish [1, 2]. In this regard, recent measurements of the *ab*-plane ( $\rho^{\parallel}$ ) and *c*-axis ( $\rho^{\perp}$ ) stiffnesses of  $\text{La}_{1.875}\text{Sr}_{0.125}\text{CuO}_4$  (LSCO) crystals by Kapon *et. al.* [3] have been puzzling. Counter to the expectation above,  $\rho^{\perp}$  was seen to vanish at  $T_c^{\perp}$ , which is about 0.64 K below the vanishing temperature  $T_c^{\parallel}$  of  $\rho^{\parallel}$ .

*Disorder* – Short range uncorrelated disorder is not expected to affect the critical behavior of a superconductor, by Harris's criterion [4]. On the other hand, the cuprates are known to be highly anisotropic layered superconductors. Layer-correlated disorder, (or a gradient in dopant concentration along the *c* axis) [5, 6], yields a distribution of  $\rho^{\parallel}$  and  $T_c^{\parallel}$ . Experimentally, such inhomogeneity is manifested by a high temperature tail of the measured  $\rho^{\parallel}$  above the average  $T_c^{\parallel}$ , while  $\rho^{\perp}$  vanishes at the lowest values of  $T_c^{\parallel}$  (see Appendix A). However,  $T_c^{\parallel}$  in Ref. [3] exhibited inhomogeneity broadening of  $\sim 0.1$  K, which is significantly below the apparent difference in  $T_c$ 's.

*Finite size effects* – An alternative proposition is that finite sample dimensions play a role. Previous Monte-Carlo simulations [7, 8] of the three dimensional XY (3dXY) model found strong effects of sample dimensions on the temperature dependent stiffness coefficients. These effects are expected to be enhanced by high anisotropy.

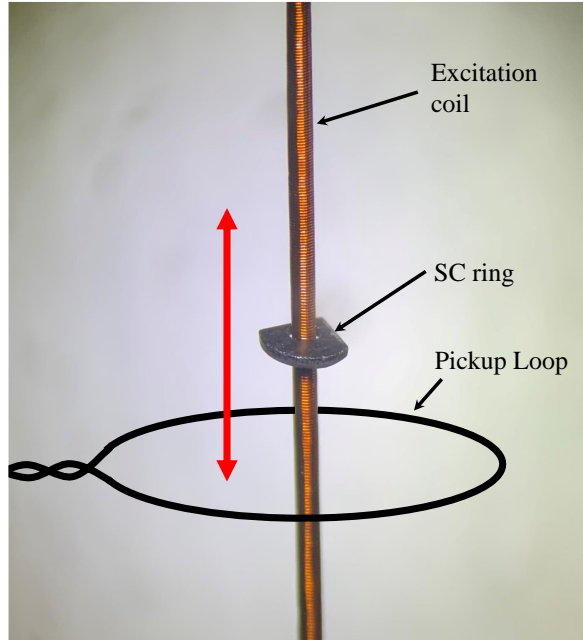


Figure 1: A superconducting ring cut in two directions, on the excitation coil. The red double arrow shows the moving direction of the schematic magnetization measuring pickup-loop, relative to both coil and ring.

This paper explores finite size effects experimentally and theoretically. We report systematic stiffness measurements near  $T_c$  for LSCO rings with widths  $L_a, L_c$  ranging between  $L = 0.1$  to 1 millimeter.  $T_c^{\parallel}$  is found to be weakly dependent on  $L_c, L_a$ . In contrast, a significant reduction of  $T_c^{\perp}$  for decreasing width  $L_a$  is observed. This behavior is not expected for layer-correlated inhomogeneity. The relatively strong finite size effect demands theoretical explanation.

Phenomenologically, the monotonous relation between  $T_c$  and  $\rho^{\parallel}$  in cuprates [9], and the observed jump in  $\rho^{\parallel}$  at  $T_c$  in ultra-thin films [10], suggest that  $T_c$  is driven by superconducting phase fluctuations [11], and vortex unbinding [12]. Therefore we appeal to the highly anisotropic layered classical 3dXY model (rather than BCS theory) to explain the stiffness temperature dependence toward  $T_c$ .

Our Monte-Carlo calculations show an apparent reduction of  $T_c^{\perp}$  with the layers' width. These results are fit to an analytical theory which combines interlayer mean field theory [13], critical behavior of the 3dXY model [1], and a crossover to the one dimensional XY (1dXY) chain [8] as temperature approaches  $T_c$ . Our theory is compared to the experimental  $T_c^{\perp}(L_a)$  in order to estimate of the anisotropy parameter of  $\text{La}_{1.83}\text{Sr}_{0.17}\text{CuO}_4$  near its thermodynamic  $T_c$ .

## 2 Experiments

Measurements were carried out with a ‘stiffnessometer’ apparatus [14] which comprises of a long excitation coil piercing a superconducting ring. A bias current in the coil creates an Aharonov-Bohm (AB) vector potential  $\mathbf{A}$  which, by London’s equation, produces a persistent current that is measured by the induced (dia-)magnetization  $m^{\alpha}$  along the coil axis  $\alpha$ . One then measures  $m^{\alpha}$  by moving a pickup loop relative to the ring and coil. The

apparatus is shown in Fig. 1.

$\text{La}_{2-x}\text{Sr}_x\text{CuO}_4$  is known to grow in large single crystals allowing significant size reductions. A bunch of crystals with different doping were grown using an image furnace, oriented with a Laue camera, and cut into rings with a femtosecond laser cutter. For each doping two rings, labelled by  $a$  and  $c$ , were prepared with their coil axes parallel ( $a$ ) and perpendicular ( $c$ ) to the  $\text{CuO}_2$  planes. The width and height of the rings was varied by the laser, or polished down to the geometries shown in Fig. 2a,b.

For the  $a$ -ring, we varied mostly the narrowest (bottleneck) widths of the  $a-b$  planes,  $L_a$ , whereas for the  $c$ -ring we varied both  $L_c$  and  $L_a$  (see Figs. 2a,b). Fig. 2(c) shows the narrowest bottleneck geometry of the  $a$ -ring. The requirement to: cut, measure, cut, measure, et cetera, the same pair of samples proved challenging. In most cases one of the samples broke during some step of the process. Only one pair of  $\text{La}_{1.83}\text{Sr}_{0.17}\text{CuO}_4$  rings survived the reduction of  $L_a$  by factor of 10 between the initial and final cutting stages. The magnetization of this sample is depicted in Fig. 2.

When the transverse London penetration depth  $\lambda_c$  ( $\lambda_a$ ) is smaller than the sample width  $L_c$  ( $L_a$ ), the induced persistent current in the superconductor precisely cancels the AB flux of the coil. This results in a temperature independent induced magnetization  $m^a$  ( $m^c$ ) at low temperatures.

As  $T \rightarrow T_c$ , the AB flux in the coil is under screened as  $\lambda_\alpha(T) \geq L_\alpha$ . In this temperature regime  $m^\alpha(T)$  decreases rapidly and becomes linearly proportional to the in-plane stiffness components. As an example, for the geometry of a perfect ring

$$\begin{aligned} m^{a,c}(T) &= h \int_{r_{\text{in}}}^{r_{\text{out}}} dr \pi r^2 (\hat{\mathbf{r}} \times \mathbf{j}_{\text{sc}}(r))^{a,c} \\ &= -h(r_{\text{out}}^2 - r_{\text{in}}^2) \frac{\Phi}{4} \rho^{\perp,\parallel}(T) \quad . \end{aligned} \quad (1)$$

$h$ ,  $r_{\text{in}}$ , and  $r_{\text{out}}$  are the ring's height, and inner and outer radii, and  $\Phi$  is the flux produced by the coil. For irregular rings extracting  $\rho^\perp, \rho^\parallel$  from  $m^\alpha(T)$  requires a full solution of Ginzburg-Landau and Bio-Savart equations [15]. However, here we do not require the magnitude of  $\rho^\perp, \rho^\parallel$  but only their vanishing temperatures  $T_c^\perp$  and  $T_c^\parallel$ . These are experimentally determined by the vanishing of the corresponding magnetizations.

Figs. 2(d,e) depict the temperature-dependent relative magnetizations  $m^\alpha(T, L_\alpha)/m_{\text{max}}^\alpha$ , for  $\alpha = a, c$ .  $m_{\text{max}}^\alpha$  is the zero temperature magnetization of the largest ring. Fig. 2(d) shows a strong dependence of the  $a$ -ring's magnetization apparent vanishing temperature  $\tilde{T}_c^\perp$  on the transverse width  $L_a$ . In contrast, the  $c$ -rings' magnetization in Fig. 2(e), exhibit insensitivity to the sample widths in the ranges  $L_a \in [1.05, 0.23]$  and  $L_c \in [0.67, 0.19]$ . We note an exception of the  $(L_a, L_c) = (0.09, 0.19)$  mm sample, which we believe to be damaged by a deep fracture during the cutting process.

We note that the  $c$ -ring magnetizations exhibit a high temperature tail of  $\simeq 0.5$  K above the extrapolated transition at  $\tilde{T}_c^\parallel$ . This is attributed to layer-correlated inhomogeneity as discussed in the Introduction and Appendix A. This inhomogeneous broadening will be taken into account in fitting theory to the experimental data in Section 3.

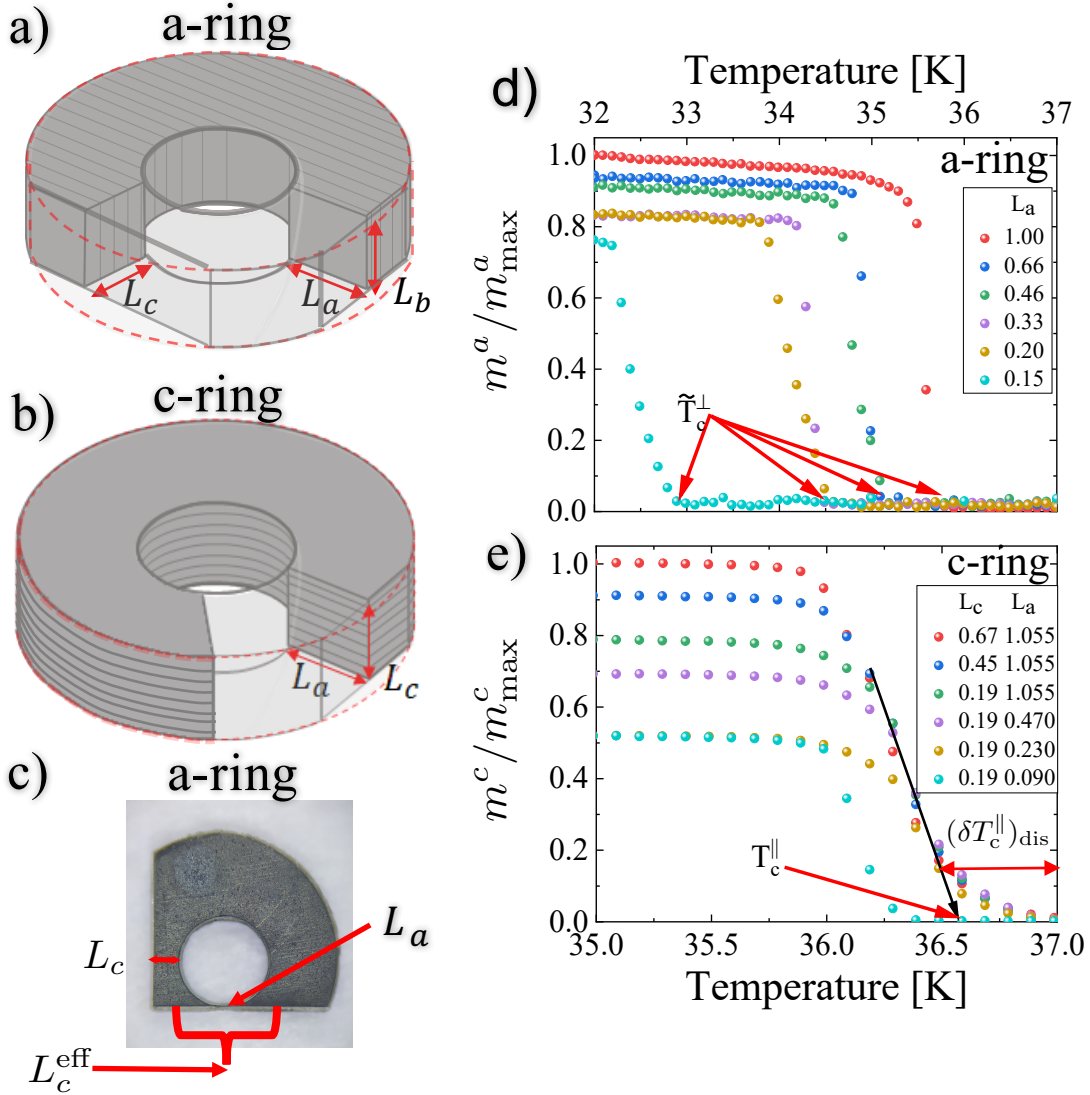


Figure 2: Experimental configuration and normalized magnetizations of  $\text{La}_{1.83}\text{Sr}_{0.17}\text{CuO}_4$  rings for a fixed 1 mA current in the coil. (a) The interior of the *a*-ring. The  $\text{CuO}_2$  planes are parallel to the ring's symmetry axis. This ring is sequentially polished to reduce the layers' width  $L_a$  in the bottleneck region. (b) The interior of the *c*-ring. The  $\text{CuO}_2$  planes are perpendicular to the ring's symmetry axis. This ring is polished along two planes which varies both  $L_a$  and  $L_c$ . (c) Photograph of an *a*-ring with two cut planes.  $L_c^{\text{eff}}$  defines the effective aspect ratio in the bottleneck region. (d) Magnetization  $m^a$  of *a*-rings with variable  $L_a$ . The apparent stiffness vanishing temperatures are denoted by  $\tilde{T}_c^\perp(L_a)$ . (e) Magnetization  $m^c$  of *c*-rings. Except for the narrowest sample  $L_a = 0.09$  (which is suspected of containing a traversing cut), the magnetizations near their transition are insensitive to  $L_a$ . The tail of width  $(\delta T_c^\parallel)_{\text{dis}} \simeq 0.5$  K is assumed to reflect some layer-correlated disorder, which is a smaller effect than the finite size dependence of the *a*-rings'  $\tilde{T}_c^\perp$ .  $\tilde{T}_c^\parallel$  is averaged in-plane transition temperature (see Section 6 and Appendix A).

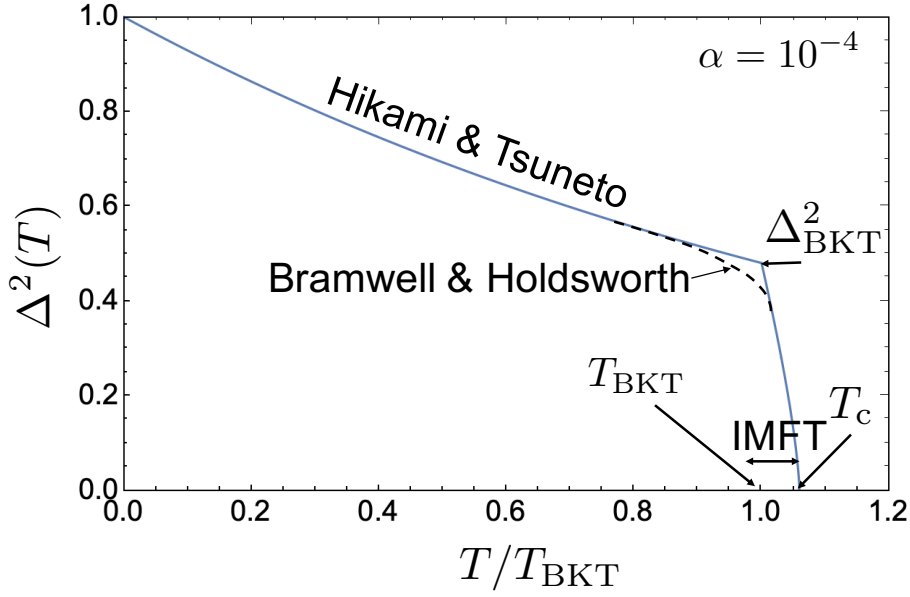


Figure 3: The order parameter squared as a function of temperature for the layered classical XY model, for anisotropy parameter  $\alpha = 10^{-4}$ . The graph patches the linear spinwave theory of Hikami and Tsuneto [21], the crossover (dashed line) power law of Bramwell and Holdsworth [18], and the three dimensional critical point which is obtained by Interplane Mean Field Theory (IMFT) of Eqs.(3), (4) and (5).

### 3 Layered 3dXY model

We model the phase fluctuations of  $\text{La}_{1.83}\text{Sr}_{0.17}\text{CuO}_4$  near  $T_c$  by the classical 3dXY Hamiltonian on a tetragonal lattice,

$$H_{3dXY} = - \sum_i \sum_{\gamma} J_{\gamma} \cos(\varphi_{\mathbf{r}_i} - \varphi_{\mathbf{r}_i + \mathbf{a}_{\gamma}}) \quad , \quad (2)$$

where  $\gamma \in \{a, b, c\}$  and where  $J_a = J_b = J^{\parallel}$  and  $J_c = J^{\perp}$  are the effective intra- and inter-plane Josephson couplings. The effective anisotropy parameter is defined as  $\alpha = J^{\perp}/J^{\parallel}$ .  $\alpha$  will later be determined to fit experimental data near  $T_c$ .

The two dimensional limit  $\alpha = 0$  reduces to the two dimensional XY (2DXY) model, where by Mermin and Wagner theorem the superconducting order parameter  $\Delta = \langle e^{i\varphi} \rangle$ , and  $\rho^{\perp}$  vanish at all temperatures. Nevertheless, the in-plane stiffness is non-zero below the Berezinskii-Kosterlitz-Thouless [12] transition at  $T_{\text{BKT}} \simeq 0.893J_a$ .

For small but finite anisotropy  $0 < \alpha \ll 1$ , interlayer mean field theory (IMFT) is very useful [13, 16–19]. It predicts  $\Delta(T) > 0$  for  $T < T_c$ , where  $T_c$  is the three dimensional critical temperature. IMFT uses the exponential divergence of the BKT susceptibility above  $T_{\text{BKT}}$  to obtain,

$$\frac{T_c(\alpha) - T_{\text{BKT}}}{T_{\text{BKT}}} = \left( \frac{b}{|\ln(0.14\alpha)|} \right)^2 \quad . \quad (3)$$

Here, the (non universal) constant is taken to be  $b = 2.725$  [20].

In the regime  $[0, T_{\text{BKT}}]$ , the order parameter magnitude  $\Delta = |\langle e^{i\varphi} \rangle|$  decreases from unity as calculated by Hikami and Tsuneto [21],

$$\Delta^2(T)_{T \leq T_{\text{BKT}}} \simeq \exp\left(-\frac{T \log(1/\alpha)}{4\pi J_a}\right) \quad . \quad (4)$$

Over the crossover regime  $T \in [T_{\text{BKT}}, T_c]$ , the order parameter squared initially crosses over with an intermediate power law of  $|T - T^*|^{0.46}$ , where  $T^* = T_{\text{BKT}} + \frac{1}{4}(T_c - T_{\text{BKT}})$  [18], above which it drops precipitously toward  $T_c$  as,

$$\Delta^2(T) = \Delta_{\text{BKT}}^2 t^{2\beta} \quad , \quad t \equiv \left( \frac{T_c - T}{T_c - T_{\text{BKT}}} \right) \quad , \quad (5)$$

where  $\beta$  crosses over from the mean field value  $\frac{1}{2}$  to the 3dXY exponent 0.349, within a narrow three dimensional Ginzburg critical region of width  $T_c/\log^4(\alpha)$  [13].

Fig. 3 depicts the smoothed “trapezoidal” temperature dependence of  $\Delta^2$  which differs from the BCS theory for the gap squared. We note that the spectral gaps observed by photoemission do not directly measure the thermodynamic order parameter. In the underdoped pseudogap phase [22], parts of the Fermi surface gap survives above  $T_c$  [23,24]. A more direct measurement of  $\Delta^2$  near  $T_c$  would be the superconducting stiffness [1, 13], since

$$\rho_\gamma(T) \propto \Delta^{2-\eta\nu\beta^{-1}} \quad (6)$$

where  $\eta$  and  $\nu$  are the critical correlation function power law and correlation length exponents respectively. For the 3dXY model  $\eta\nu = 0.0255$  which is small and henceforth neglected.

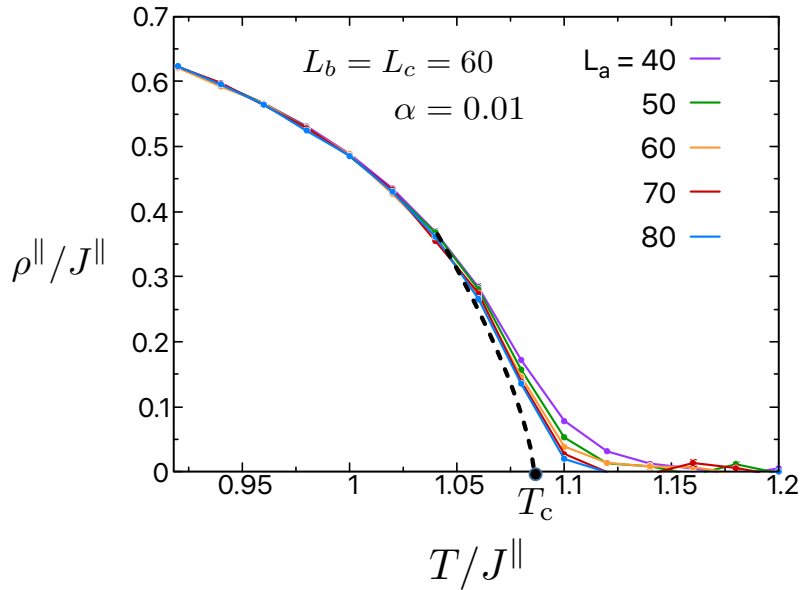


Figure 4: The intra-plane stiffness  $\rho^{\parallel}$ , plotted as a function of temperature  $T$ , for  $\alpha = 0.01$  and for different  $L_a$  between 40 and 80, while  $L_b$  and  $L_c$  are kept fixed at 60. The error bars are smaller than the point sizes. The black dashed line shows the critical behavior near the thermodynamic transition temperature  $T_c$ , according to Eq. (6).

## 4 Monte Carlo simulations

The superfluid stiffness (*i.e.* helicity modulus) of Eq. 2 with  $a_\gamma = 1$ , is given by [7, 25]

$$\rho_\gamma = \frac{J_\gamma}{V} \left\langle \sum_{\langle ij \rangle} \cos(\varphi_{\mathbf{r}_i} - \varphi_{\mathbf{r}_j}) (r_i^\gamma - r_j^\gamma)^2 \right\rangle - \frac{J_\gamma^2}{VT} \left\langle \left( \sum_{\langle ij \rangle} \sin(\varphi_{\mathbf{r}_i} - \varphi_{\mathbf{r}_j}) (r_i^\gamma - r_j^\gamma) \right)^2 \right\rangle, \quad \gamma = a, b, c. \quad (7)$$

$V = L_a L_b L_c$ . The first contribution measures the short range correlations, which are proportional to minus the energy along the bonds in the  $\gamma$  direction. The second contribution measures long range current fluctuations, which vanish at zero temperature, and reduce the stiffness at finite temperatures.

We compute Eq. (7) by a Monte Carlo (MC) simulation of  $H_{3dXY}$  with the Wolff cluster updates algorithm [26], see Appendix D for details. We choose  $L_c = L_b = 60$ , and vary the width in the range  $L_a \in \{40, 50, \dots, 80\}$  using the anisotropy parameters in the range  $\alpha = 0.01 - 0.02$ . The minimal accessible anisotropy parameter is determined by the maximal lattice size.

In Fig. 4, we plot the intra-plane stiffness  $\rho^\parallel$  as a function of temperature  $T$ , and width  $L_a$ . The anisotropy parameter is fixed at  $\alpha = 0.01$ .  $T_c \simeq 1.086$ . The expected thermodynamic critical behavior, Eq. (6), is depicted by a dashed line in Fig. 4. For the disorder-free model, the tail above  $T_c$  indicates that the in-plane correlation length exceeds  $L_a$ . Thus, a larger  $L_a$  reduces the width of the tail. For millimeter scale superconducting rings, this tail should be unobservably small.

In Fig. 5, the MC data for  $\rho^\perp(T)$  are shown as points. Given a numerical resolution threshold  $\varepsilon$ ,  $\rho^\perp(T)$  appears to vanish at transition temperatures  $\tilde{T}_c^\perp$  which depend on  $\varepsilon$  and the width  $L_a$ . The solid lines and the inset describe a fit of the MC data to analytic formulas derived in the following Section.

## 5 Crossover to one dimensional Josephson array

The *apparent* premature vanishing of  $\rho^\perp$  in a finite size sample of an approximately unit aspect ratio, is due to its crossover to a quasi one-dimensional behavior as  $T \rightarrow T_c$ . The stiffness of a one dimensional (1d) Josephson array with inter-grain couplings  $J_{1d}$ , lattice constant  $a$  and chain length  $L$  is

$$\rho_{1d}(T, L) = TLZ_2/Z_0 \quad (8)$$

$$Z_{2p} = \sum_{n=-\infty}^{\infty} \left( \frac{I_n(J_{1d}/T)}{I_0(J_{1d}/T)} \right)^{L/a} n^{2p},$$

where  $I_n$  are modified Bessel functions and  $p = 0, 1$ . Luttinger liquid (LL) theory [8, 27], which applies at  $L \gg a$ , yields an analytic result where  $\rho_{1d}$  depends on the dimensionless variable  $x \equiv LT/(J_{1d}a)$  as,

$$\rho_{LL}(J_{1d}, x) = J_{1d} a \left( 1 - \frac{\pi^2 \vartheta_3''(0, e^{-2\pi^2/x})}{x \vartheta_3(0, e^{-2\pi^2/x})} \right) \quad (9)$$

$$\simeq J_{1d} a \begin{cases} 1 & (x \leq 2) \\ 20 \exp(-0.472 x) & (x \geq 10) \end{cases},$$

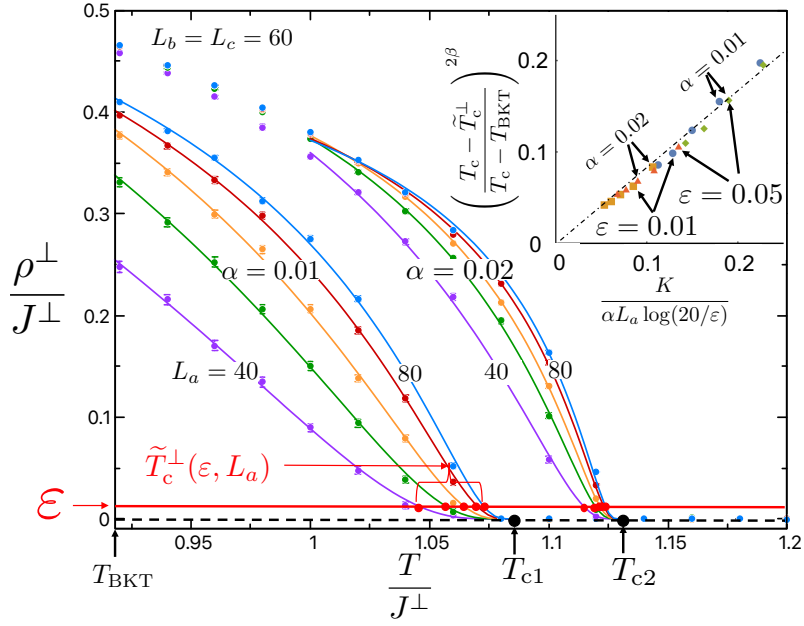


Figure 5: MC evaluations of  $\rho^\perp$  for the clean 3dXY model Eq. (2), a function of temperature for a range of sample widths  $L_a \in \{40, 50, \dots, 80\}$ , and anisotropy parameters  $\alpha$ . The thermodynamic critical temperatures are evaluated as  $T_{c1} = 1.086J_a$  and  $T_{c2} = 1.13J_a$  for  $\alpha = 0.01$  and  $0.02$ , respectively. Solid lines are best fits to Eq. (12).  $\varepsilon$  is arbitrarily chosen as the numerical resolution which defines the apparent transition temperatures  $\tilde{T}_c^\perp$  by Eq. (14). Inset: Verification of Eq. (15) by collapse of all the temperature shifts for various  $L_a, \varepsilon, \alpha$  obtained from the main graphs.

where  $\vartheta_3(z, q) = 1 + 2 \sum_{n=1}^{\infty} q^{n^2} \cos(2nz)$ , and prime denotes differentiation with respect to  $z$ . Comparison between Eqs. (8) and (9) is shown in Appendix B.

Now we return to the  $c$ -axis stiffness  $\rho^\perp$  of the layered model (2), which can be described as a chain of Josephson junctions along the  $c$ -axis with inter-grain coupling,

$$J_{\text{eff}}(T) = \frac{L_a L_b}{(\xi^\parallel)^2} \times J^\perp \Delta^2(T), \quad (10)$$

Toward  $T_c$ ,  $\Delta^2(T)$  vanishes as  $t^{2\beta}$  by Eq. (5). Substituting  $J_{1d} = J_{\text{eff}}(T)$  we expect the asymptotic behavior of Eq. (9) to be realized by after replacing

$$x \rightarrow \frac{L_c T}{J_{\text{eff}}(T) \xi^\perp}. \quad (11)$$

Thus for  $t \ll 1$ ,  $x \gg 1$  and

$$\rho^\perp(T) \approx 20 \rho^\perp(T_{\text{BKT}}) \exp\left(-\frac{K}{\alpha L_a} t^{-2\beta}\right), \quad (12)$$

$$K \simeq \frac{0.472 r T_c (\xi^\parallel)^2}{J_a \Delta_{\text{BKT}}^2 \xi^\perp}. \quad (13)$$

For any experimental resolution  $\varepsilon$ , an apparent vanishing temperature  $\tilde{T}_c^\perp(\varepsilon)$  is defined by the threshold condition,

$$\frac{\rho^\perp(\tilde{T}_c^\perp)}{\rho^\perp(T_{\text{BKT}})} = \varepsilon. \quad (14)$$



By Eq. (12), the apparent width dependent transition temperature is,

$$T_c - \tilde{T}_c^\perp = (T_c - T_{\text{BKT}}) \left( \frac{K}{\alpha L_a \log(20/\varepsilon)} \right)^{1/2\beta} \quad (15)$$

The most important consequence of the quasi one-dimensional behavior, is that the temperature shifts are proportional to  $(\alpha L_a)^{-1/2\beta}$ . This is a much larger shift than expected from critical fluctuations, which are of order  $(\alpha L_a^2)^{-1}$ .

In the inset of Fig. 5 we verify the validity of Eq. (15) by collapsing of all the temperature shifts onto a straight line. The slope of this line differs only by 20% from unity, which we attribute to the choice of the (non-universal) constants in the asymptotic expression of Eq. (9).

## 6 Comparison of Theory to Experiments

In comparing Eq. 15 to the MC results, we have used the 3dXY critical exponent  $\beta = 0.349$ .

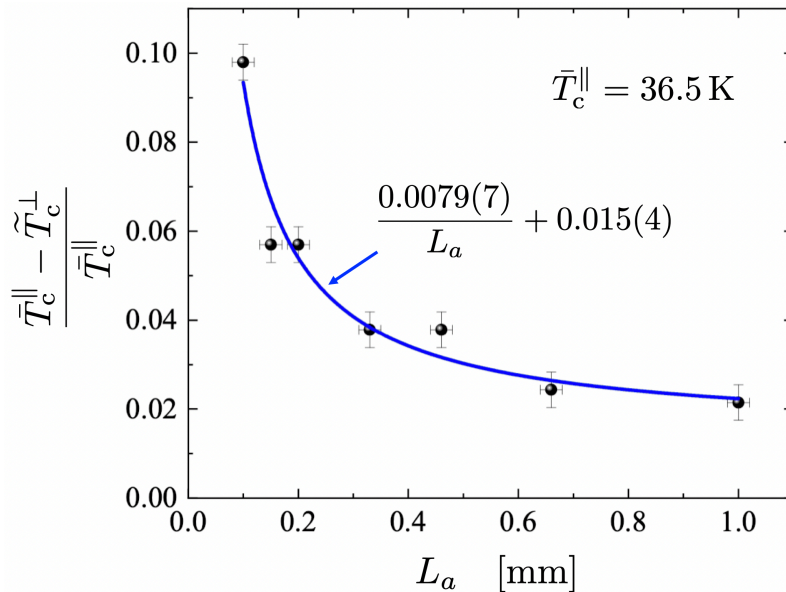


Figure 6: Comparison of experimental results for  $\text{La}_{1.83}\text{Sr}_{0.17}\text{CuO}_4$  rings of Fig. 2 and theoretical prediction of Eqs. (15) and (19). Crosses: The apparent  $c$ -axis transition temperature shifts  $\tilde{T}_c^\perp$  of the  $a$ -rings, as determined in Fig. 2(d).  $L_a$  are the bottleneck widths of the  $ab$  planes. Line: the least square fit using  $\alpha^{\text{fit}} = 4.1 \times 10^{-5}$ . The offset of the reduced temperature 0.015(4) agrees with the estimated layer-correlated disorder (see text). We use the mean field exponent  $\beta = \frac{1}{2}$ , due to the narrow Ginzburg critical regime near  $T_c$ .

For the experimental LSCO crystals, the millimeter width corresponds to  $\sim 10^5$  effective lattice constants, and the anisotropy parameter will turn out to be  $\alpha < 10^{-4}$ , which yields an unobservable narrow Ginzburg critical region. Hence we shall fit the Eq. 15 with the mean field exponent  $\beta = 0.5$ .

The  $a$ -ring is sequentially cut such that the induced current is governed by the bottleneck region. There the induced current flows in along the  $c$  axis over an effective length of

$L_c^{\text{eff}} = 2$  mm. The transverse dimension  $L_b = 0.46$  mm yields  $r = 4.34$ . The width is varied in the range  $L_a \in [0.1, 1]$  mm. We estimate the experimental resolution at  $\varepsilon = 10^{-2}$ . (High accuracy of  $\varepsilon$  is not essential, since  $\tilde{T}_c^\perp$  depends on it logarithmically).

At zero temperature the coherence lengths have been determined experimentally [28] to be  $\xi^\parallel(0) \simeq 3$  nm and  $\xi^\perp(0) \simeq 1.3$  nm. The in-plane lattice constant for the effective 3dXY model is the coherence length estimated at  $T_{\text{BKT}}$  to be  $\xi^\parallel(T_{\text{BKT}}) = \xi^\parallel(0)/\Delta_{\text{BKT}}$ . Due to the incoherent single-electron tunneling between the layers, we assume that the Cooper pair size in the  $c$  direction remains confined to a single plane  $\xi^\perp(T_{\text{BKT}}) \simeq \xi^\perp(0)$ .

In Fig. 6, the apparent  $c$ -axis transition temperatures  $\tilde{T}_c^\perp(L_a)$  are plotted. The data is somewhat noisy, presumably because of the introduction of deep cuts during the ring's cutting process, which are eliminated by subsequent cuts. The two-parameter fit function is plotted,

$$\frac{\bar{T}_c^\parallel - \tilde{T}_c^\perp}{\bar{T}_c^\parallel} = \frac{A}{L_a[\text{mm}]} + (\delta t)_{\text{dis}} \quad (16)$$

with  $A = 0.0079$  and  $(\delta t)_{\text{dis}} = 0.015(4)$ . The dimensionless temperature shift  $(\delta t)_{\text{dis}}$  is understood as the effect of layer-correlated inhomogeneity (see Appendix A). We use the high temperature tail of magnitude  $(\delta T_c^\parallel)_{\text{dis}} \simeq 0.5$  K, which is depicted in Fig. 2(e). Subtracting  $(\delta T_c^\parallel)_{\text{dis}}$  from  $\bar{T}_c^\parallel = 36.5$  K yields a bound for  $\tilde{T}_c^\perp$  for wide samples,

$$\lim_{L_a \rightarrow \infty} \tilde{T}_c^\perp = \bar{T}_c^\parallel - (\delta T_c^\parallel)_{\text{dis}} = 36 \text{ K}. \quad (17)$$

The estimated layer-correlated disorder shift is consistent with the fit in Fig. 6,

$$(\delta t)_{\text{dis}} \equiv \frac{(\delta T_c^\parallel)_{\text{dis}}}{\bar{T}_c^\parallel} \in 0.015(4). \quad (18)$$

Using Eqs. (3), (4), (13) and (15), and the parameters listed above we obtain

$$A = \Delta T_c(\alpha) \frac{0.472 \times 10^{-6} r T_c (\xi^\parallel)^2}{\alpha \Delta_{\text{BKT}}^4(\alpha) \xi^\perp \log(20/\varepsilon)} = 0.0079 \quad (19)$$

which can be fit by the anisotropy parameter,

$$\alpha^{\text{fit}}(T \simeq T_c) = 4.1 \times 10^{-5} \quad (20)$$

## 7 Discussion and Summary

We note that  $\alpha^{\text{fit}}$  parametrizes the effective Hamiltonian near  $T_c$ . We can compare it to the anisotropy parameter reported by that obtained for optimally doped LSCO (for  $\text{Sr}_{0.15}$ ) at zero temperature in Ref. [29],

$$\alpha^\lambda(T=0) = \left(\frac{\lambda_c}{\lambda_a}\right)^{-2} = 4.6 \times 10^{-3}. \quad (21)$$

The difference in anisotropy can be attributed to the reduction of interplane coherence due to thermally excited nodal quasiparticles of the  $d$ -wave superconductor and the effects of interplanar vortex rings above the two dimensional  $T_{\text{BKT}}$ .

*Analog in  $^4\text{He}$*  – We have seen that  $\alpha \ll 1$  can be mapped onto an isotropic model on samples with large aspect ratio. A similar “premature” vanishing of  $\rho^\perp$  has been observed on a quasi-one dimensional brick, *i.e.*  $L_a \ll L_c$  [7]. This result was used to

explain the experimental disappearance of superfluid density of  $^4\text{He}$  embedded in quasi one-dimensional nanopores [30, 31]. Here we explain the *apparent* reduction of  $\tilde{T}_c(L_a)$ , not as a true thermodynamic transition but rather as a consequence of an essential singularity decay of  $\rho^\perp$  toward the thermodynamic  $T_c$ .

In conclusion, layered superconductors with high anisotropy may exhibit a large difference between the apparent transition temperatures of in-plane and out of plane persistent currents. Below  $T_c$ , finite sample width results in a crossover to one dimensional behavior near  $T_c$ , where the inter-layer critical current is exponentially suppressed below the thermodynamic  $T_c$ .

We mention that emergent anisotropy of layered superconductors has been an important consequence of certain pair density wave ordering [32]. We propose that the dependence of inter-layer stiffness transition temperatures on sample width could help characterize the emergent anisotropy parameter near  $T_c$ .

## 8 Acknowledgements

A.S. and I.M. contributed equally to this work. We thank Erez Berg, Snir Gazit, Dror Orgad, and Daniel Podolsky for beneficial discussions. AA acknowledge the Israel Science Foundation (ISF) Grant No. 2081/20. A.K. acknowledges the ISF Grant. No. 1251/19 and 3875/21. This work was performed in part at the Aspen Center for Physics, which is supported by National Science Foundation grant PHY-2210452, and at the Kavli Institute for Theoretical Physics, supported by Grant Nos. NSF PHY-1748958, NSF PHY-1748958 and NSF PHY-2309135.

## A Planar correlated disorder

Refs. [5, 6] have considered the layered  $XY$  model where the  $ab$  planes exhibit a variable  $z$ -dependent stiffness  $\rho^\parallel(z)$  for  $z \in [0, L_c]$ . We can see the effects of bounded correlated disorder on superconductors with a variation of  $\rho^\parallel(z)$  along the  $c$ -axis. In each segment, the stiffness temperature dependence has a different  $T_c$ ,

$$\rho^\parallel(T) = \rho^\parallel(0) \left| \frac{T - T_c^\parallel(z)}{\bar{T}_c^\parallel} \right|^{2\beta - \eta\nu} \quad (22)$$

where  $T_c^\parallel(z) \propto \rho^\parallel(z, 0)$  is the local transition temperature whose average is defined as  $\bar{T}_c^\parallel$  and maximal variation is  $(\delta T_c^\parallel)_{\text{dis}}$ . The global  $ab$ -stiffness is given by the integral

$$\rho^\parallel = \rho^\parallel(0) \int_0^{L_c} \frac{dz}{L_c} \left| \frac{T - T_c^\parallel(z)}{\bar{T}_c^\parallel} \right|^{2\beta - \eta\mu}, \quad (23)$$

which smears the average critical temperature  $\bar{T}_c^\parallel$  by a high temperature tail at  $T \in [\bar{T}_c^\parallel, \bar{T}_c^\parallel + (\delta T_c^\parallel)_{\text{dis}}]$ .

In contrast, the  $c$ -axis stiffness  $\rho^\perp(z)/\rho^\perp(0)$  is proportional to the local order parameter squared  $\Delta(z) \propto |T - T_c(z)|^\beta$ . The global  $c$ -axis stiffness is the harmonic average given by,

$$\rho^\perp = \rho^\perp(0) \left( \int_0^{L_c} \frac{dz}{L_c} \frac{(\bar{T}_c^\parallel)^{2\beta}}{|T - T_c^\parallel(z)|^{2\beta}} \right)^{-1}. \quad (24)$$

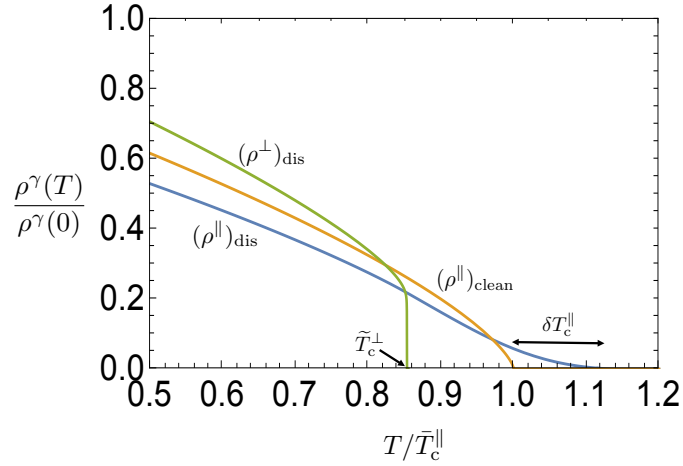


Figure 7: Effects of planar-correlated disorder, modelled by  $c$ -axis dependent in-plane stiffness  $\rho^\parallel(z)$ , with an average transition temperature  $\bar{T}_c^\parallel$  and a width of transition temperatures  $(\delta T_c^\parallel)_{\text{dis}} = 0.1\bar{T}_c^\parallel$ . Orange line: The clean system with a three dimensional critical behavior. Blue line: the global  $\rho^\parallel$  showing a disorder induced high temperature tail above  $\bar{T}_c^\parallel$ . Green line: the global  $\rho_\perp^{\text{dis}}$ , which is dominated by the weakest interplane stiffnesses, and vanishes below  $T_c^\parallel$ .

The weakest segment, with the lowest  $\rho^\perp(z)$ , dominates the integral. The temperatures where the order parameter of this segment vanishes is

$$\tilde{T}_c^\perp \leq \bar{T}_c^\parallel - (\delta T_c^\parallel)_{\text{dis}} \quad , \quad (25)$$

above which the global  $\rho^\perp(T)$  disappears. The effect of bounded layer-correlated disorder is demonstrated in Fig. 7.

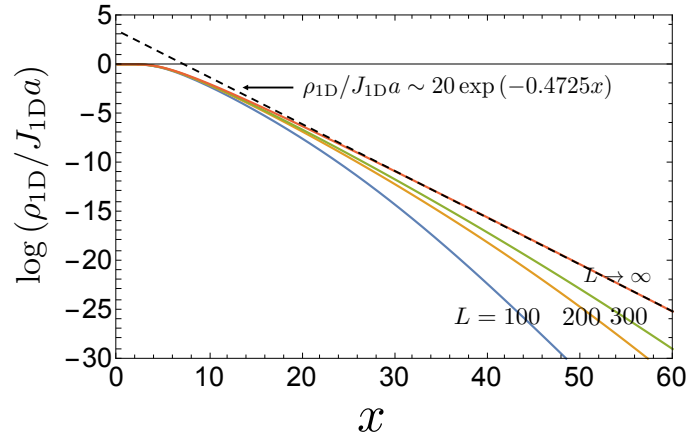


Figure 8: Stiffness as a function of scaled variable  $x = LT/(J_{1D}a)$  in the one dimensional XY model for different lengths  $L$  as given by the exact result of Eq. (7), and asymptotically at  $L \rightarrow \infty$  by Eq. (8) of the main text.

## B Asymptotic behavior of stiffness of a one dimensional XY chain

In Fig. 8 we depict the exact result of the stiffness of the one dimensional XY chain as given by Eq. (7) of the main text. At large  $L/a$  the graphs show convergence to the analytic Luttinger-Liquid form [8, 27], which at large  $x$  is given by Eq. (8) of the main text.

## C Estimation of finite size shift in $T_c$

Fine size scaling produce unobservably small finite size shifts of  $T_c$  for millimeter size samples, as shown by the following. The correlation lengths above  $T_{\text{BKT}}$  diverge as

$$\xi^{\parallel}(t) \simeq \frac{1}{\sqrt{\alpha}} \xi_a^{(0)} t^{-\nu} \quad , \quad \xi^{\perp}(t) \simeq \xi_c^{(0)} t^{-\nu} \quad (26)$$

where we use the Ginzburg Landau definition of correlation lengths,  $\xi_{\gamma}^{-1} \propto \sqrt{\rho_{\gamma}}$ , to obtain the factor of  $\sqrt{\alpha}$  between the divergent correlation length.

For Eq. (2) with sample dimensions  $L_{\gamma}, \gamma = a, b, c$  the stiffness components near  $T_c$  vanish as [33],

$$\frac{\rho_c}{\rho_c(T_{\text{BKT}})} = t^{\nu} \Phi[x_a] \quad , \quad x_a = \xi_a(t)/L_a. \quad (27)$$

where  $\Phi(x)$  is differentiable function with a finite value at  $x = 0$ . We expand  $\Phi$  to linear order in  $\xi_a$  and set  $\rho^{\perp} \rightarrow 0$  to obtain,

$$0 = \Phi_0 + \partial_{x_a} \Phi \times \left( \frac{t^{-\nu} \xi_a^{(0)}}{\sqrt{\alpha} L_a} \right) + \mathcal{O}(x_a^2) \quad (28)$$

which is solved by a positive shift of  $T_c$  by the amount

$$\delta t \simeq - \frac{\Phi_0}{\partial_a \Phi_{\gamma}} \left( \frac{\sqrt{\alpha} L_a}{\xi_a^{(0)}} \right)^{-1/\nu}. \quad (29)$$

For the experimental  $\text{La}_{1.83}\text{Sr}_{0.17}\text{CuO}_4$  rings, taking  $\alpha = 10^{-5}$ ,  $L_a/\xi_a^{(0)} \sim 10^6$ , yields  $|\delta t| \leq 10^{-4}$ , which is much below experimental temperature resolution.

## D Details of the Monte-Carlo simulations using cluster algorithm

The superfluid stiffness or the helicity modulus (with  $a_{\gamma} = 1$ ) for the classical Hamiltonian of Eq. (2) is given by Eq. (7) [7, 25, 34].

In the Wolff-cluster algorithm [26], we assume the XY spins  $\mathbf{S}$  to be the unit vectors in  $\mathbb{R}^3$ . In every monte-carlo (MC) step, we first choose a random site  $\mathbf{r} \in \mathbb{R}_3$  and a random direction  $\mathbf{d} \in S_2$ , and consider a reflection of the spin on that site about the hyperplane orthogonal to  $\mathbf{d}$ . Note that this is equivalent to the spin-flipping operation in Ising model. We then travel to all neighboring sites ( $\mathbf{r}'$ ) of  $\mathbf{r}$ , and check if the bond  $\langle \mathbf{r} \mathbf{r}' \rangle$  is activated with a probability

$$P_{\gamma}(\mathbf{r}, \mathbf{r}') = 1 - \exp\left(\min[0, 2J_{\gamma}\beta(\mathbf{d} \cdot \mathbf{S}_{\mathbf{r}})(\mathbf{d} \cdot \mathbf{S}_{\mathbf{r}'})]\right), \quad (30)$$

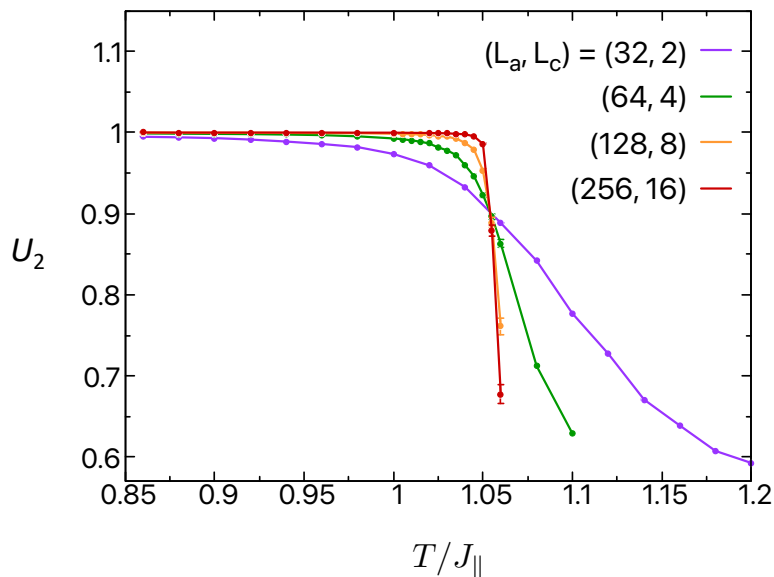


Figure 9: Binder cumulant  $U_2$  plotted as a function of temperature  $T$ , for anisotropy  $\alpha = 0.005$  and for different sizes with a fixed aspect ratio  $L_a/L_c = 16$  and  $L_b = L_a$ .

where  $\beta$  is the inverse temperature. If this satisfies, we mark  $\mathbf{r}'$  and include it to a cluster  $\mathcal{C}$  of “flipped” spins. We iteratively continue this process for all unmarked neighboring sites of  $\mathbf{r}'$  and grow the cluster size until all the neighbors turn out to be marked. We use such  $10^6$  number of MC steps for thermalization, followed by another  $10^7$  number of MC steps for measurement of different observables, such as the helicity modulus and the binder cumulant. We estimate the errors of different observables by using a standard Jackknife analysis of the MC data.

In Fig. 3 of the main text, we have presented the inter-plane superfluid stiffness  $\rho^\perp$  for different system sizes of  $L_a \in [60 - 80]$ ,  $L_b = L_c = 60$ , near the transition.

Next we calculate the Binder cumulant, defined in terms of the higher powers of magnetization  $m$  as following [35]

$$U_2 = \frac{3}{2} \left( 1 - \frac{1}{3} \frac{\langle m^4 \rangle}{\langle m^2 \rangle^2} \right), \quad (31)$$

and we use it to extract the value of critical temperatures accurately. As an example, in Fig. 9, we present  $U_2$  as a function of  $T$ , for an anisotropy parameter  $\alpha = 0.005$  and for different system sizes with a fixed aspect ratio  $L_a = L_b$  and  $L_a/L_c = 16$ . In the ordered phase when all the spins are aligned it takes a value 1, while in the disordered phase it vanishes and takes an intermediate value between 0 and 1 at the critical point. Therefore, by tracking the crossing between different system sizes, we find a critical temperature  $T_c \sim 1.05$  for these parameters. using a similar analysis, we obtain  $T_c$  for other anisotropy parameters also, discussed in the main text.

## References

- [1] M. E. Fisher, M. N. Barber and D. Jasnow, *Helicity Modulus, Superfluidity, and Scaling in Isotropic Systems*, Phys. Rev. A **8**, 1111 (1973), doi:10.1103/PhysRevA.8.1111.

- [2] M. Hasenbusch, *Monte Carlo study of an improved clock model in three dimensions*, Phys. Rev. B **100**, 224517 (2019), doi:10.1103/PhysRevB.100.224517.
- [3] I. Kapon, Z. Salman, I. Mangel, T. Prokscha, N. Gavish and A. Keren, *Phase transition in the cuprates from a magnetic-field-free stiffness meter viewpoint*, Nat. Comm. **10**(1), 2463 (2019), doi:10.1038/s41467-019-10480-x.
- [4] A. B. Harris, *Effect of random defects on the critical behaviour of Ising models*, Jour. Phys. C: Sol. State Phys. **7**(9), 1671 (1974).
- [5] P. Mohan, P. M. Goldbart, R. Narayanan, J. Toner and T. Vojta, *Anomalously elastic intermediate phase in randomly layered superfluids, superconductors, and planar magnets*, Phys. Rev. Lett. **105**(8), 085301 (2010).
- [6] D. Pekker, G. Refael and E. Demler, *Finding the Elusive Sliding Phase in the Superfluid-Normal Phase Transition Smeared by  $c$ -Axis Disorder*, Phys. Rev. Lett. **105**, 085302 (2010), doi:10.1103/PhysRevLett.105.085302.
- [7] A. Kotani, K. Yamashita and D. S. Hirashima, *Superfluid density in quasi-one-dimensional systems*, Phys. Rev. B **83**, 174515 (2011), doi:10.1103/PhysRevB.83.174515.
- [8] D. S. Hirashima, *Helicity modulus of the quasi-one-dimensional XY model: Protection by an energy barrier*, Phys. Rev. B **102**(10), 104506 (2020).
- [9] Y. J. Uemura, G. M. Luke, B. J. Sternlieb, J. H. Brewer, J. F. Carolan, W. N. Hardy, R. Kadono, J. R. Kempton, R. F. Kiefl, S. R. Kreitzman, P. Mulhern, T. M. Riseman *et al.*, *Universal Correlations between  $T_c$  and  $n_s/m^*$  in High- $T_c$  Cuprate Superconductors*, Phys. Rev. Lett. **62**, 2317 (1989), doi:10.1103/PhysRevLett.62.2317.
- [10] I. Hetel, T. R. Lemberger and M. Randeria, *Quantum critical behaviour in the superfluid density of strongly underdoped ultrathin copper oxide films*, Nat. Phys. **3**(10), 700 (2007).
- [11] V. J. Emery and S. A. Kivelson, *Importance of phase fluctuations in superconductors with small superfluid density*, Nature **374**(6521), 434 (1995), doi:10.1038/374434a0.
- [12] J. M. Kosterlitz and D. J. Thouless, *Ordering, metastability and phase transitions in two-dimensional systems*, Jour. Phys. C: Sol. State Phys. **6**(7), 1181 (1973).
- [13] A. Mihlin and A. Auerbach, *Temperature dependence of the order parameter of cuprate superconductors*, Phys. Rev. B **80**(13), 134521 (2009).
- [14] I. Mangel, I. Kapon, N. Blau, K. Golubkov, N. Gavish and A. Keren, *Stiffnessometer: A magnetic-field-free superconducting stiffness meter and its application*, Phys. Rev. B **102**(2), 024502 (2020).
- [15] N. Gavish, O. Kenneth and A. Keren, *Ginzburg-Landau model of a stiffnessometer—A superconducting stiffness meter device*, Physica D: Nonlinear Phenomena **415**, 132767 (2021).
- [16] D. J. Scalapino, Y. Imry and P. Pincus, *Generalized Ginzburg-Landau theory of pseudo-one-dimensional systems*, Phys. Rev. B **11**(5), 2042 (1975).
- [17] B. Keimer, A. Aharony, A. Auerbach, R. J. Birgeneau, A. Cassanho, Y. Endoh, R. W. Erwin, M. A. Kastner and G. Shirane, *Néel transition and sublattice magnetization of pure and doped  $La_2CuO_4$* , Phys. Rev. B **45**, 7430 (1992).

- [18] S. T. Bramwell and P. C. W. Holdsworth, *Magnetization: A characteristic of the Kosterlitz-Thouless-Berezinskii transition*, Phys. Rev. B **49**, 8811 (1994), doi:10.1103/PhysRevB.49.8811.
- [19] P. Butera and M. Pernici, *Extended scaling behavior of the spatially anisotropic classical XY model in the crossover from three to two dimensions*, Phys. Rev. B **80**, 054408 (2009), doi:10.1103/PhysRevB.80.054408.
- [20] J. M. Kosterlitz, *The critical properties of the two-dimensional XY model*, Jour. Phys. C: Sol. State Phys. **7**(6), 1046 (1974).
- [21] S. Hikami and T. Tsuneto, *Phase transition of quasi-two dimensional planar system*, Prog. Theor. Phys. **63**(2), 387 (1980).
- [22] S. Hübner, M. Hossain, A. Damascelli and G. Sawatzky, *Two gaps make a high-temperature superconductor?*, Reports on Progress in Physics **71**(6), 062501 (2008).
- [23] W.-S. Lee, I. Vishik, K. Tanaka, D. Lu, T. Sasagawa, N. Nagaosa, T. Devereaux, Z. Hussain and Z.-X. Shen, *Abrupt onset of a second energy gap at the superconducting transition of underdoped  $Bi2212$* , Nature **450**(7166), 81 (2007).
- [24] A. Kanigel, U. Chatterjee, M. Randeria, M. Norman, S. Souma, M. Shi, Z. Li, H. Raffay and J. Campuzano, *Protected nodes and the collapse of fermi arcs in high- $T_c$  cuprate superconductors*, Physical review letters **99**(15), 157001 (2007).
- [25] S. Teitel and C. Jayaprakash, *Phase transitions in frustrated two-dimensional XY models*, Phys. Rev. B **27**, 598 (1983), doi:10.1103/PhysRevB.27.598.
- [26] U. Wolff, *Collective Monte Carlo Updating for Spin Systems*, Phys. Rev. Lett. **62**, 361 (1989), doi:10.1103/PhysRevLett.62.361.
- [27] A. Del Maestro and I. Affleck, *Interacting bosons in one dimension and the applicability of Luttinger-liquid theory as revealed by path-integral quantum Monte Carlo calculations*, Phys. Rev. B **82**, 060515 (2010), doi:10.1103/PhysRevB.82.060515.
- [28] I. Mangel and A. Keren, *The Ground-state Inter-plane Superconducting Coherence Length of  $La_{1.875}Sr_{0.125}CuO_4$  Measured by a "Xiometer"*, arXiv:2308.06757 .
- [29] C. Panagopoulos, J. Cooper, T. Xiang, Y. Wang and C. Chu, *c-axis superfluid response and pseudogap in high- $T_c$  superconductors*, Physical Review B **61**(6), R3808 (2000).
- [30] N. Wada, J. Taniguchi, H. Ikegami, S. Inagaki and Y. Fukushima, *Helium-4 Bose fluids formed in one-dimensional 18 diameter pores*, Phys. Rev. Lett. **86**(19), 4322 (2001).
- [31] R. Toda, M. Hieda, T. Matsushita, N. Wada, J. Taniguchi, H. Ikegami, S. Inagaki and Y. Fukushima, *Superfluidity of  $He_4$  in One and Three Dimensions Realized in Nanopores*, Phys. Rev. Lett. **99**(25), 255301 (2007).
- [32] D. F. Agterberg, J. S. Davis, S. D. Edkins, E. Fradkin, D. J. Van Harlingen, S. A. Kivelson, P. A. Lee, L. Radzihovsky, J. M. Tranquada and Y. Wang, *The physics of pair-density waves: Cuprate superconductors and beyond*, Annual Review of Condensed Matter Physics **11**(1), 231 (2020), doi:10.1146/annurev-conmatphys-031119-050711, <https://doi.org/10.1146/annurev-conmatphys-031119-050711>.



- [33] Y.-H. Li and S. Teitel, *Finite-size scaling study of the three-dimensional classical XY model*, Phys. Rev. B **40**, 9122 (1989).
- [34] F. Hrahsheh and T. Vojta, *Anomalous elasticity in a disordered layered XY model*, Phys. Scripta **2012**(T151), 014074 (2012).
- [35] A. W. Sandvik, *Computational studies of quantum spin systems*, In *AIP Conference Proceedings*, vol. 1297, pp. 135–338. American Institute of Physics (2010).